Conley-Morse persistence barcode

Tamal K. Dey,
Michał Lipiński,
Manuel Soriano-Trigueros

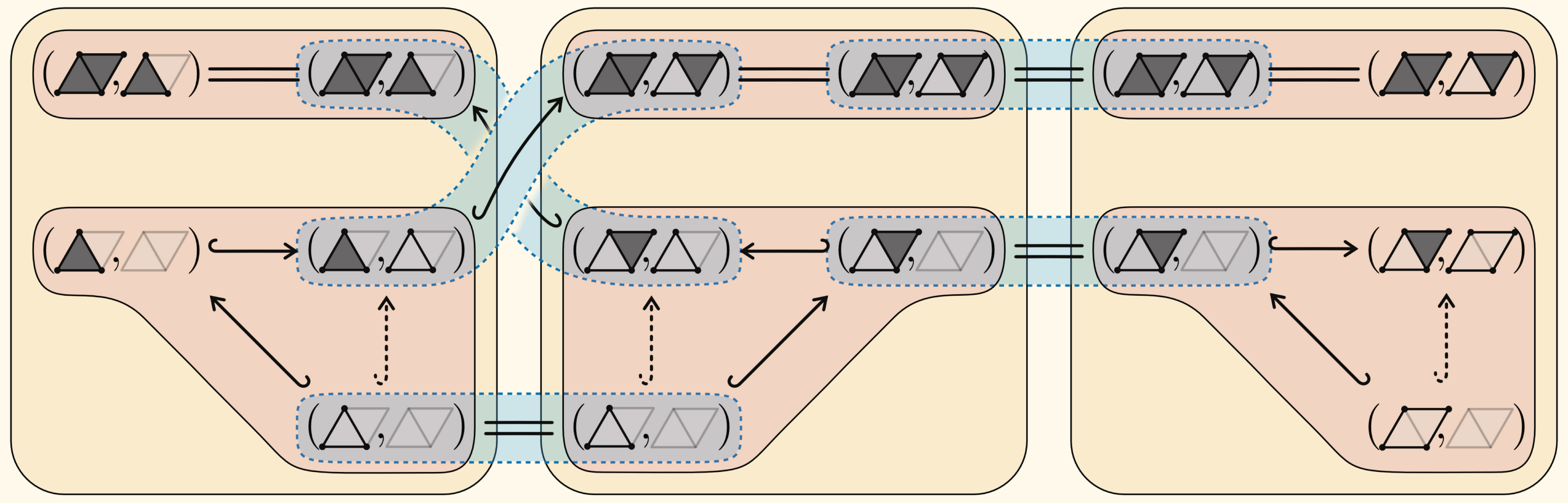

$\mathcal{B}_0 \sqsupseteq \mathcal{B}_1$ $\mathcal{B}_1 \sqsubseteq \mathcal{B}_2$ $\mathcal{B}_2 \sqsubseteq \mathcal{B}_3$

Why might this be of interest to the AATRN community?

Dynamical constraints naturally give rise to a persistence module over a poset of a specific structure, enabling its interval decomposition.

Institute of Science and Technology Austria

Main question:

How to capture the nature of a bifurcation with persistent homology?

parameterized vector field on a 2-sphere

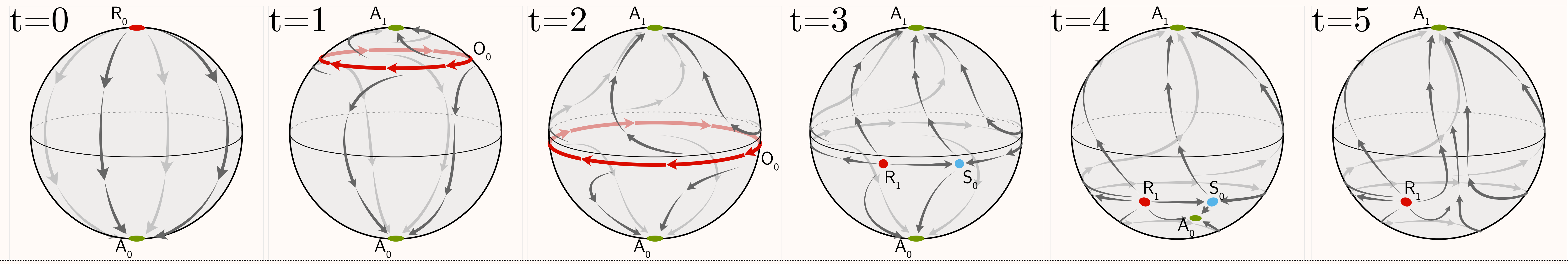

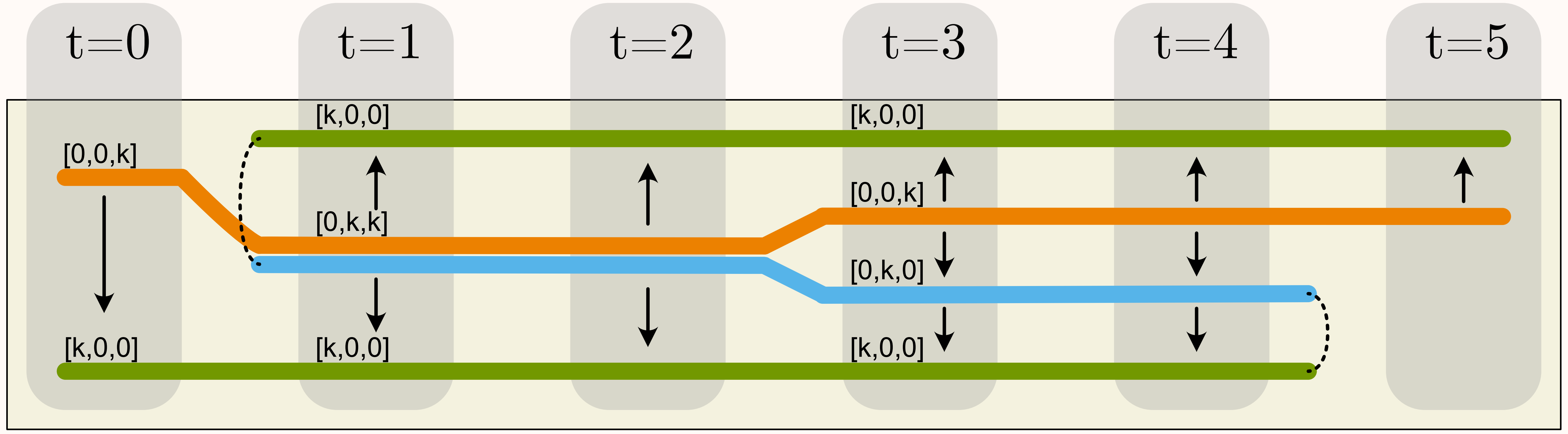

Conley-Morse persistence barcode

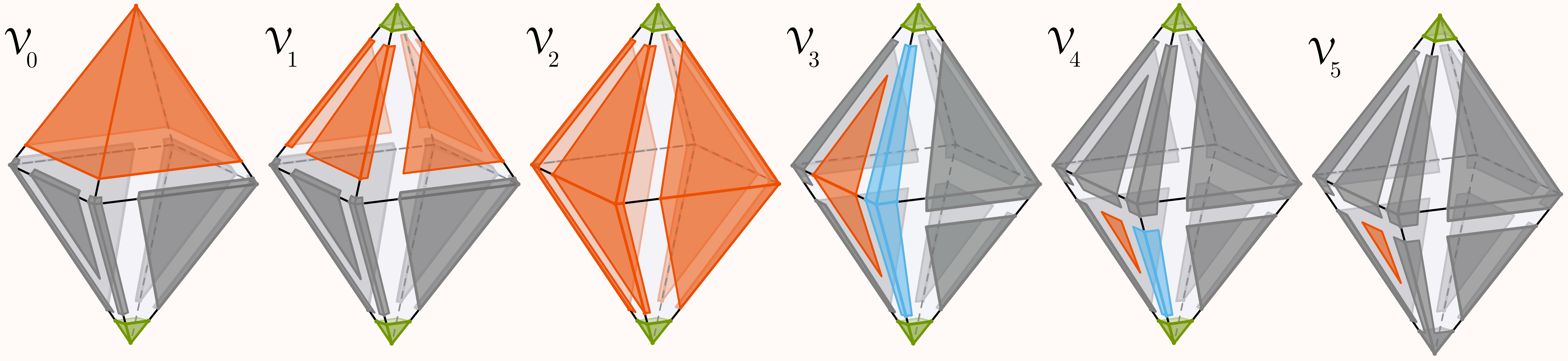

combinatorial model of the continuous vector field

Bounding the interleaving distance on concrete categories using a loss function

Astrid A. Olave H.* & Elizabeth Munch

A **generalized persistence module** is a functor $F : P \to C$ from any poset P to any category C.

Take $F, G : P \to C$. A $\mathcal{T}_\varepsilon$**-assignment** of F and G is a collection of morphisms (ϕ, ψ),

$$\phi_p : F(p) \to G\mathcal{T}_\varepsilon(p) \qquad \psi_p : G(p) \to F\mathcal{T}_\varepsilon(p)$$

Consider the following diagrams

$$\begin{tikzcd}
F(p) \arrow[r, "{F[p\leq q]}"] \arrow[dr, "\phi_p"'] & F(q) \arrow[dr, "\phi_q"] & \\
& G(\mathcal{T}_\varepsilon p) \arrow[r, "{G[\leq]}"'] & G(\mathcal{T}_\varepsilon q)
\end{tikzcd}
\qquad
\begin{tikzcd}
& F(\mathcal{T}_\varepsilon p) \arrow[r, "{F[\leq]}"] & G(\mathcal{T}_\varepsilon q) \\
G(p) \arrow[ur, "\psi_p"] \arrow[r, "{G[\leq]}"'] & G(q) \arrow[ur, "\psi_q"'] &
\end{tikzcd}$$

$$\begin{tikzcd}
F(p) \arrow[rr, "{F[p\leq \mathcal{T}_\varepsilon\mathcal{T}_\varepsilon p]}"] \arrow[dr, "\phi_p"'] & & F(\mathcal{T}_\varepsilon\mathcal{T}_\varepsilon p) \\
& G(\mathcal{T}_\varepsilon p) \arrow[ur, "\psi_{\mathcal{T}_\varepsilon p}"'] &
\end{tikzcd}
\qquad
\begin{tikzcd}
& F(\mathcal{T}_\varepsilon p) \arrow[dr, "\phi_{\mathcal{T}_\varepsilon p}"] & \\
G(p) \arrow[ur, "\psi_p"] \arrow[rr, "{G[p\leq \mathcal{T}_\varepsilon\mathcal{T}_\varepsilon p]}"'] & & G(\mathcal{T}_\varepsilon\mathcal{T}_\varepsilon p)
\end{tikzcd}$$

We define a **loss function** $L(\phi, \psi)$ that quantifies how far all diagrams are from being commutative.

(AO, Munch, E. 2025+)

Take $\varepsilon > 0$ and choose a (ϕ, ψ) a $\mathcal{T}_\varepsilon$- assignment of F and G, if $d_I(F, G)$ is their interleaving distance then

$$d_I(F, G) \leq \varepsilon + L(\phi, \psi)$$

Question: Can we use this framework to bound the interleaving distance between multiparameter persistence modules in **polynomial time** ?

HYPERBLOCK BARCODES: A ROBUST HOMOLOGICAL FEATURE FOR HYPERGRAPHS

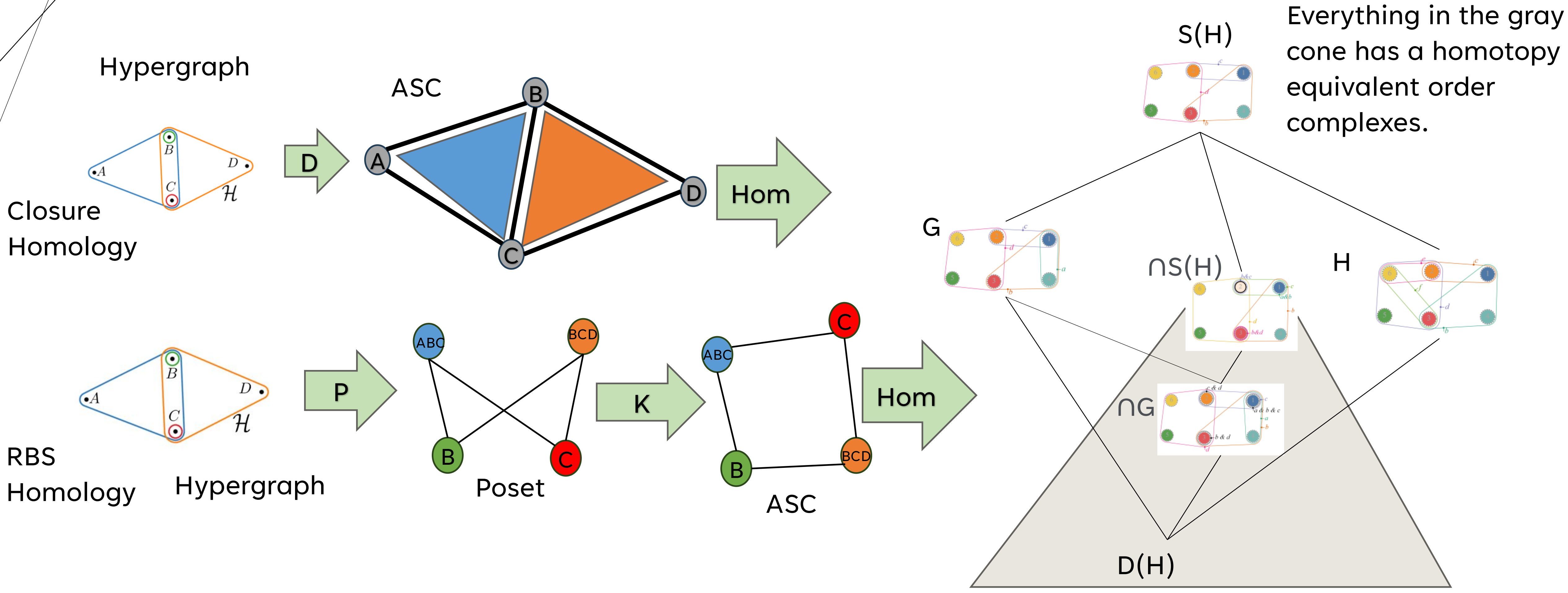

Schauder Bases for Multiparameter Persistence

Zachariah Ross
Advisor: Peter Bubenik
University of Florida: Department of Mathematics

Multiparameter Persistence Diagrams in a Polyhedral Pair

Persistence Module $M : \mathbb{R}^d \to vect$

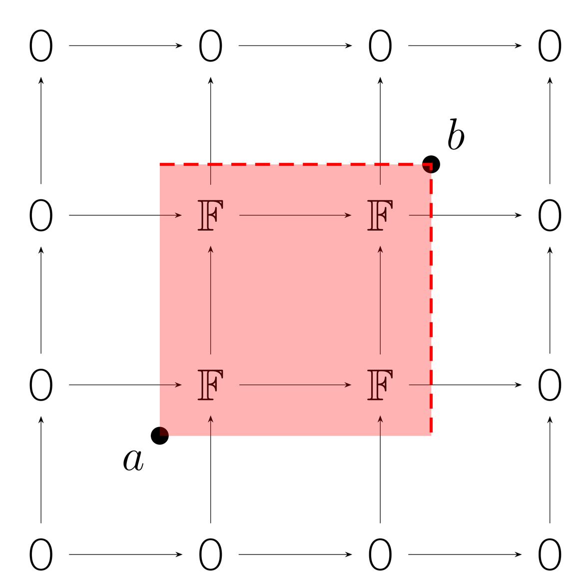

Example: Rectangle Module $\langle a, b\rangle$

$\mathcal{I} = \{rectangles\ \langle a, b\rangle \mid a < b \in \mathbb{R}^d\}$

$RK_{\mathcal{I}}(M) : \mathcal{I} \to \mathbb{Z}_+$

$I \mapsto Rank(\lim_{\leftarrow} M|_I \to \lim_{\rightarrow} M|_I)$

Signed Barcodes

Theorem (Botnan, Opperman, & Oudot): For finitely presented $M : \mathbb{R}^d \to vect$, there exists a unique minimal set of rectangles decomposing $RK_{\mathcal{I}}$, with multiplicities matching Möbius inversion of $RK_{\mathcal{I}}(M)$

Möbius Inversion of $RK_{\mathcal{I}}(M)$

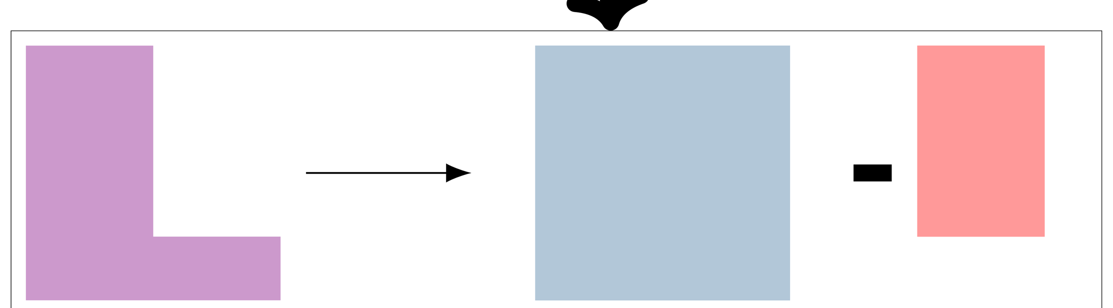

Encode rectangles in $\mathbb{R}^{2d}$

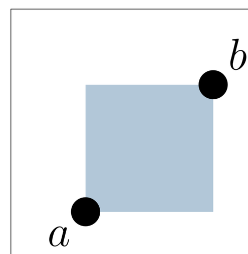

$(a_1, a_2 ... a_d, b_1 ... b_d) \in \mathbb{R}^{2d}_{\leq}$

$\mathbb{R}^{2d}_{\leq} = \{(a, b) \mid a_i \leq b_i\ \forall i\}$

Modulo Δ^d of rectangles for which $\exists i\ s.t.\ a_i = b_i$

Vectorization ???

Motivation: Statistics, Machine Learning, Functional Analysis

Banach or Hilbert space
Example: Sequence in ℓ^1: $[0.17, 0.04, 0.0, 0.01, 0.0, ...]$

Our Method

Properties:

• stable • doesn't loose information • adaptive to different experiments

Setup:

(I) Signed Barcodes encoded in a polyhedral pair (X, A)

Example: Polyhedral pair $(\mathbb{R}^2_{\leq}, \Delta)$ and $(\mathbb{R}^{2n}_{\leq}, \Delta^n)$

(II) Nested sequence of triangulations of (X, A)

(III) A set of p.l. functionals on (X, A) determined by the nested triangulation

Piece-wise Linear Functionals

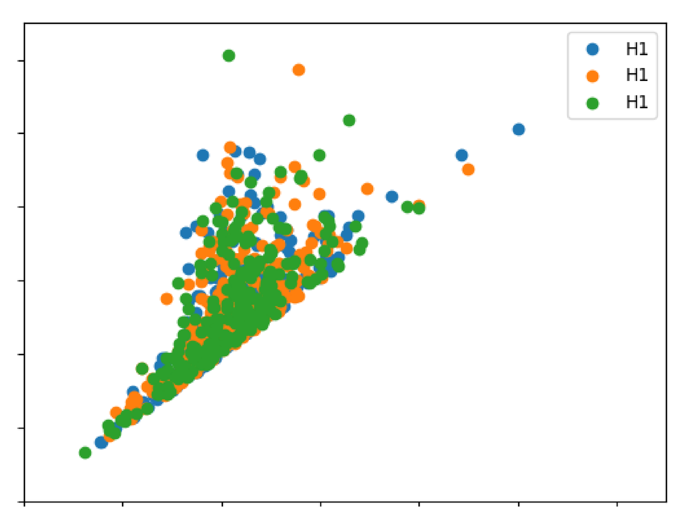

Choose Triangulation of X to "fit" training data, and iteratively refine

Define P.L. functionals by vertices of each refinement

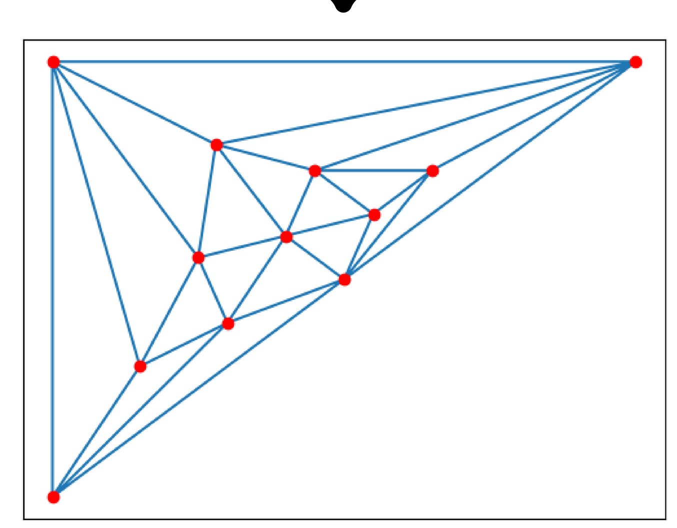

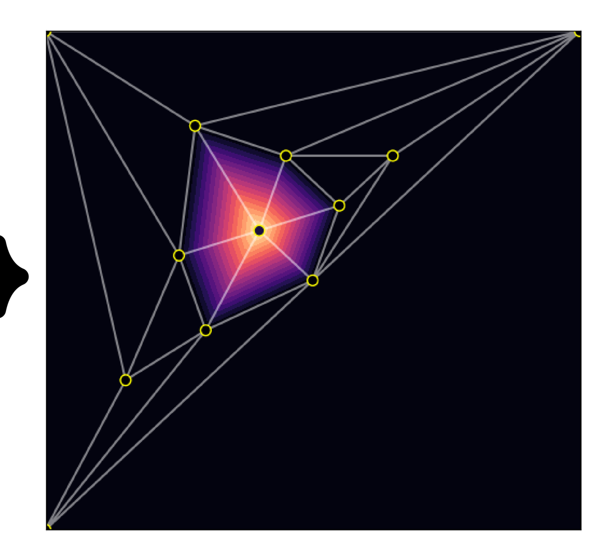

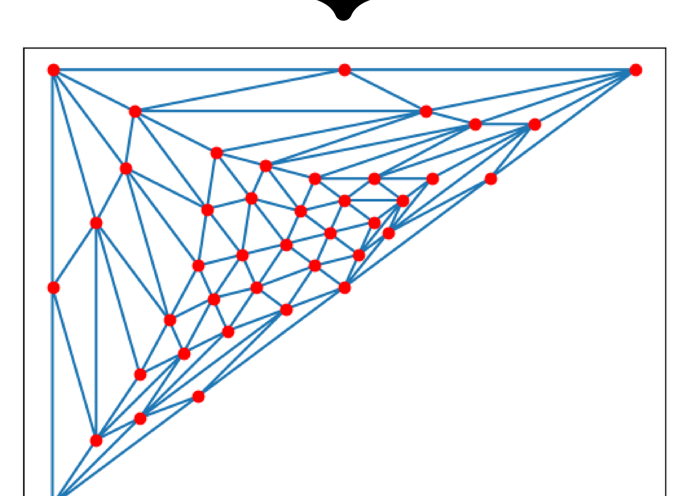

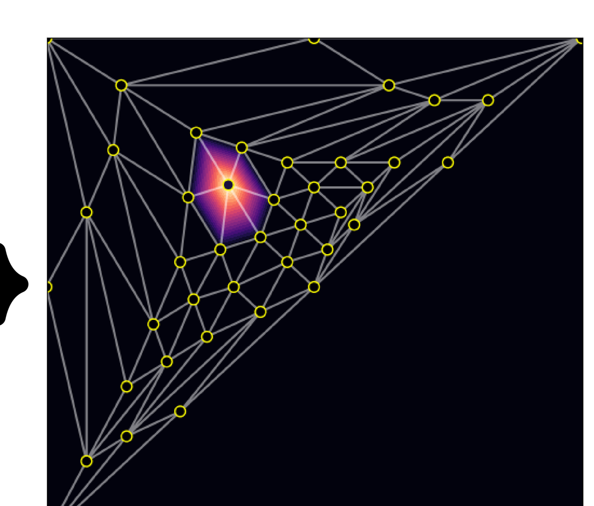

...

Schauder Basis of Compactly Supported, Lipschitz Functionals

(IV) Def: For V a topological vector space; $\mathbb{B} = \{e_i\}_{i=0}^{\infty} \subset V$ is a Schauder Basis of V if $\forall v \in V$, there exists unique $(a_i)_{i=0}^{\infty}$ such that

$$\sum_{i=0}^{\infty} a_i e_i = v$$

Theorem (R): For a polyhedral pair (X, A) **(I)**, and nested triangulation, $\mathcal{T} = \{T^p\}_{p=0}^{\infty}$ **(II)**, the corresponding sequence of p.l. functionals $\mathbb{B} = \{\mathcal{K}_i\}_{i=0}^{\infty}$ **(III)** form a Schauder Basis **(IV)** of compactly supported Lipschitz functionals on (X, A).

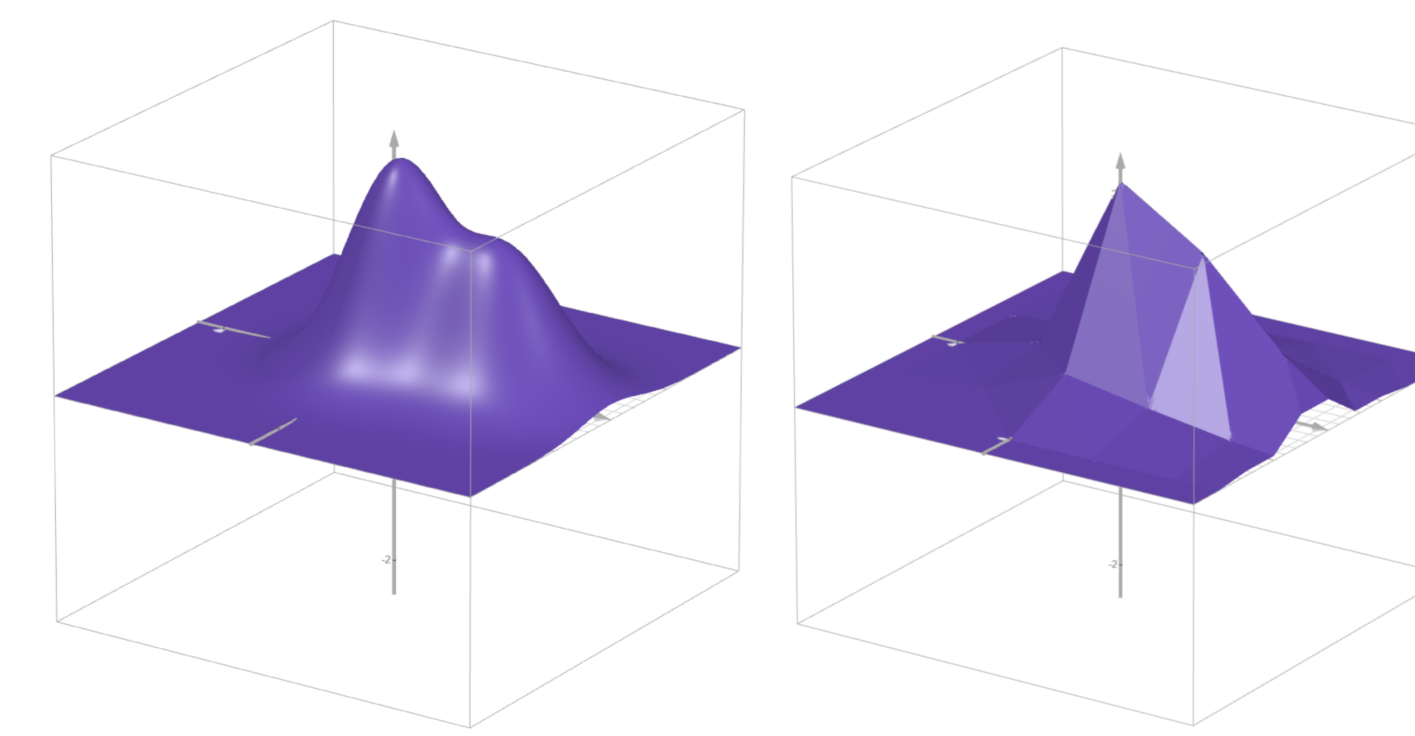

Vectorization

Extending work by Perea, Munch, and Khasawneh, we consider the following.

(V) Def: For a Schauder basis $\mathbb{B} = \{\mathcal{K}_i\}_{i=0}^{\infty}$ of compactly supported Lipschitz functionals, the induced map takes signed barcodes encoded in (X, A) to a sequence of real numbers by evaluating the barcode by each functional of $\mathbb{B}$.

$$\alpha \mapsto (\mathcal{K}_i(\alpha))_i$$

Theorem (R): Given Polyhedral pair (X, A) **(I)** and a nested triangulation $\mathcal{T}$ **(II)**, let $\mathbb{B}$ be the induced Schauder Basis of p.l. functionals **(IV)**. Then the induced mapping **(V)** is linear, injective, and Lipschitz with respect to the 1-Wasserstein distance on signed barcodes.

References

- Magnus Bakke Botnan, Steffen Oppermann, and Steve Oudot. Signed Barcodes for Multi-Parameter Persistence via Rank Decompositions and Rank-Exact Resolutions. 2024. arXiv: 2107.06800 [math.AT]. url: https://arxiv.org/abs/2107.06800.
- Perea, J.A., Munch, E. & Khasawneh, F.A. Approximating Continuous Functions on Persistence Diagrams Using Template Functions. Found Comput Math 23, 1215–1272 (2023). https://doi.org/10.1007/s10208-022-09567-7

thomas.z@ufl.edu

Topology of Molecular Braids

Riya Dogra (joint work with Dr. Senja Barthel)
r.dogra@vu.nl

Chemical Problem

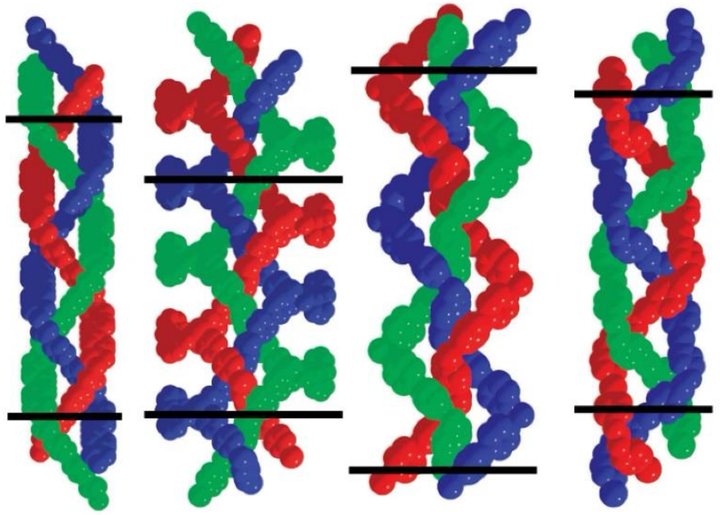

- Self-interweaving of n-molecules
- Infinite periodic structures
- Chain components start and end in the same position
- Strands are rigidly identical
- Mutually entangled, high symmetry

Mathematical Solution

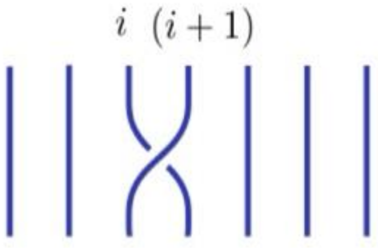

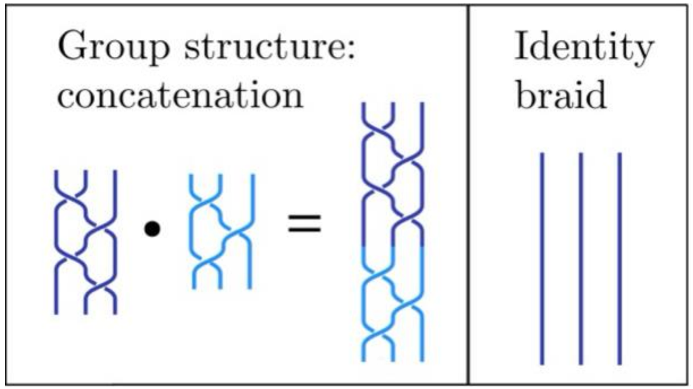

$$\begin{bmatrix} -1 & -1 \\ -1 & -1 \\ -1 & -1 \end{bmatrix}$$

- n-stranded geometric braids
- Finite braids considered upto conjugation
- Periodic unit is pure
- Minimal crossing number, n(n-1)
- Braid closures should be non-split

Towards an Optimal Bound for the Interleaving Distance on Mapper Graphs

Erin Wolf Chambers[1], *Ishika Ghosh*[2], Elizabeth Munch[2], Sarah Percival[3], Bei Wang[4]

[1]University of Notre Dame, [2]Michigan State University, [3]University of New Mexico, [4]University of Utah

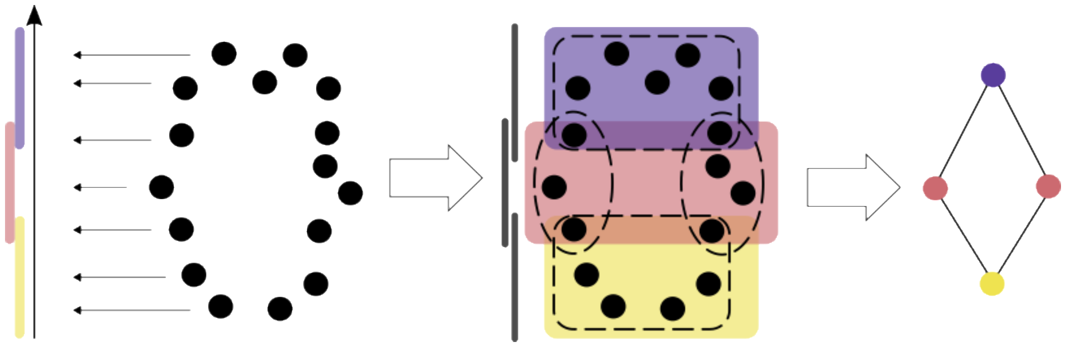

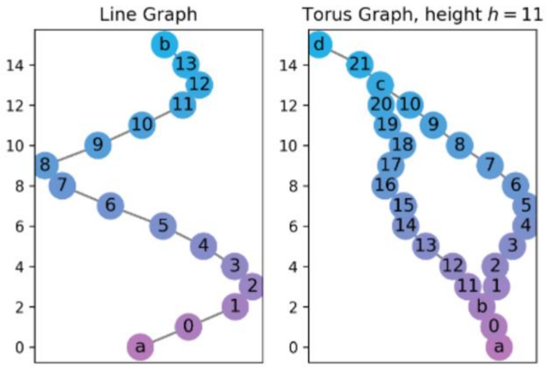

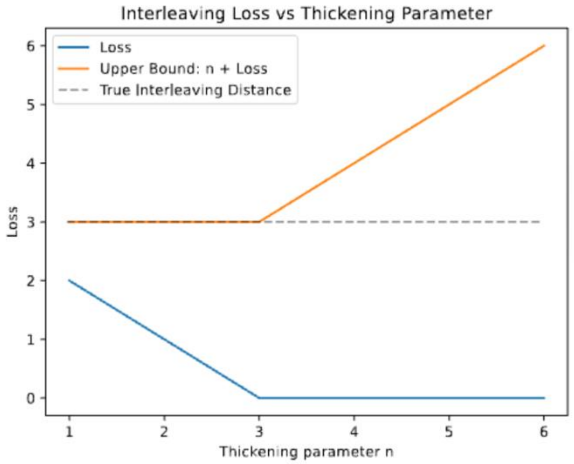

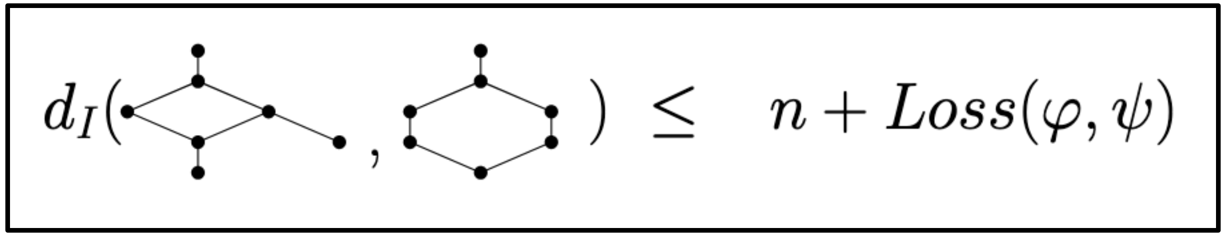

Pre-print:

Estimating Persistent Homology of $\mathbb{R}^n$-Valued Functions Using Function-Geometric Multifiltrations

Ethan André, Jingyi Li, David Loiseaux, and Steve Oudot

Setting: X compact metric space, $f : X \to \mathbb{R}^n$ (both unknown).

Input: $f|_P$ for some finite sample $P \subseteq X$ with known pairwise distances.

Construct a new persistence module M from P and $f|_P$.

Goal: estimate the $\boxed{\text{persistent homology of } f}$ from $\boxed{P \text{ and } f|_P}$.

$H_*(\mathcal{F}) : \mathbb{R}^n \to \mathrm{Vec}$, where $\mathcal{F} : \mathbb{R}^n \to \mathrm{Top}$ is a sublevel filtration of f.

Approximate $H_*(\mathcal{F})$ using M $\Rightarrow$

construction of M, theoretical guarantees, robustness to noise in the input, algorithm to compute M, statistical properties, experiments...

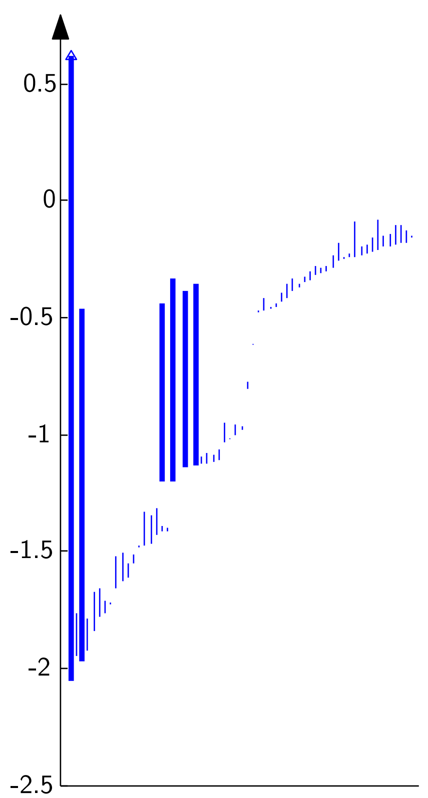

H_0

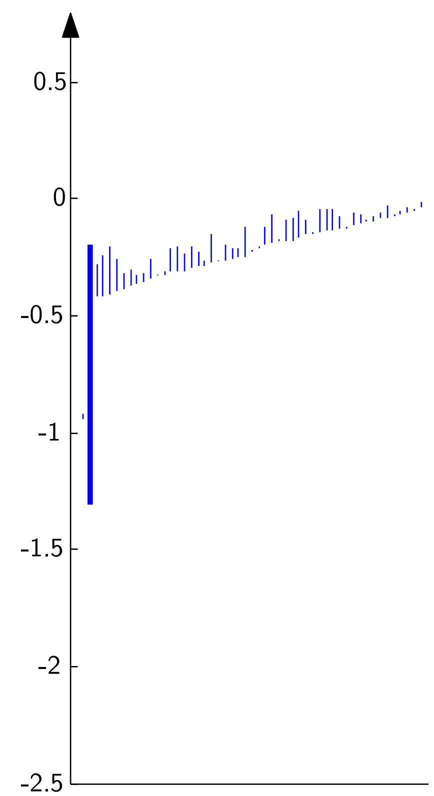

H_1

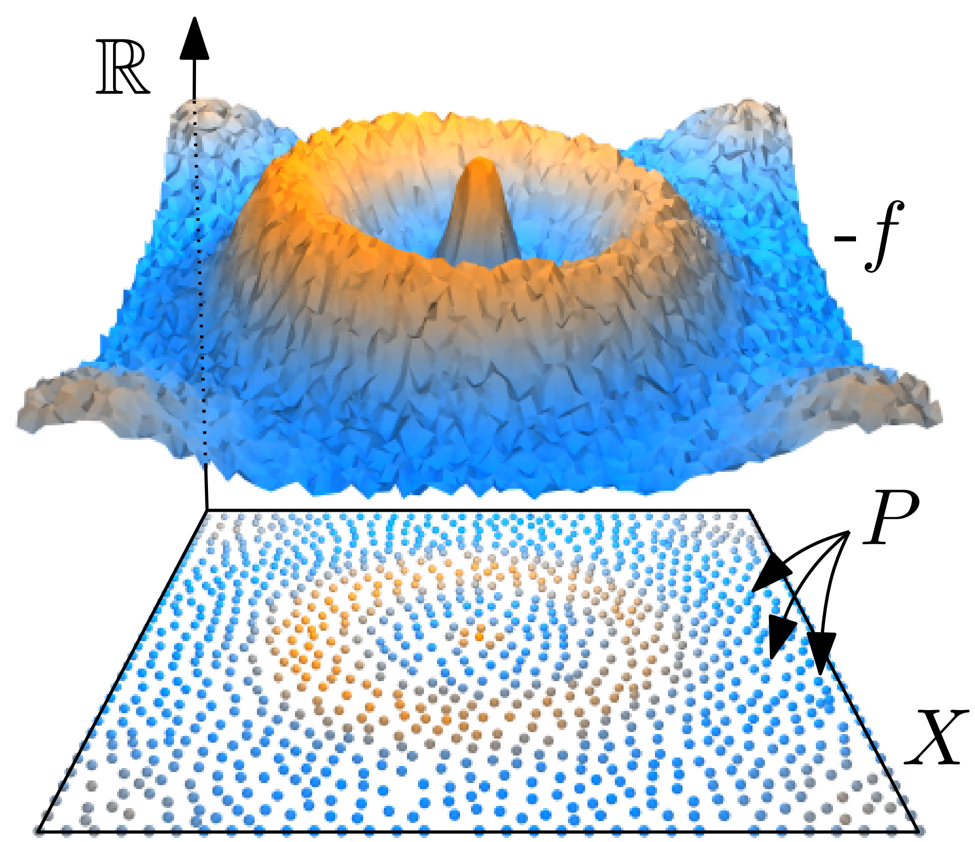

Morse Theory for Chromatic Delaunay Triangulations

A. N., Thomas Chaplin, Adam Brown, and Maria-Jose Jimenez

University of Oxford Mathematical Institute

Setup: $X \subset \mathbb{R}^d$ and labelling $\mu : X \to \{0, \dots, s\}$.

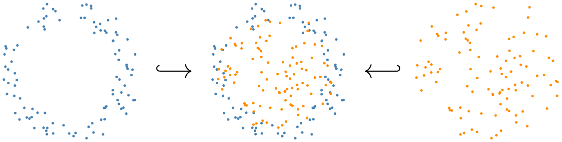

Spatial relations in data $\approx$ maps between filtrations $\approx$ induced maps on persistent homology.

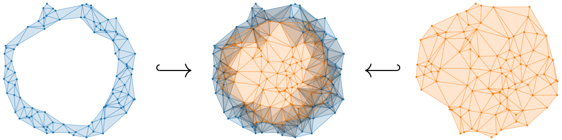

- Čech and Vietoris–Rips filtrations have too many simplices.
- Alpha filtration not functorial with respect to inclusion of points.

Chromatic Alpha Filtrations Stable, efficient in low dimensions, and recover the "right" barcode.

Our contributions:

- Filtration radius of family of related filtrations is discrete Morse.
- Underlying simplicial complex with Čech filtration values: same simple homotopy type and barcodes.
- Justification for using Rips filtration values.

Sebastiano Cultrera di Montesano et al. (2025). "Chromatic Alpha Complexes". In: *Foundations of Data Science*. DOI: 10.3934/fods.2025003

#9 Generalized cluster algorithms for Potts lattice gauge theory

Paul Duncan, **Anthony E. Pizzimenti**, and Ben Schweinhart

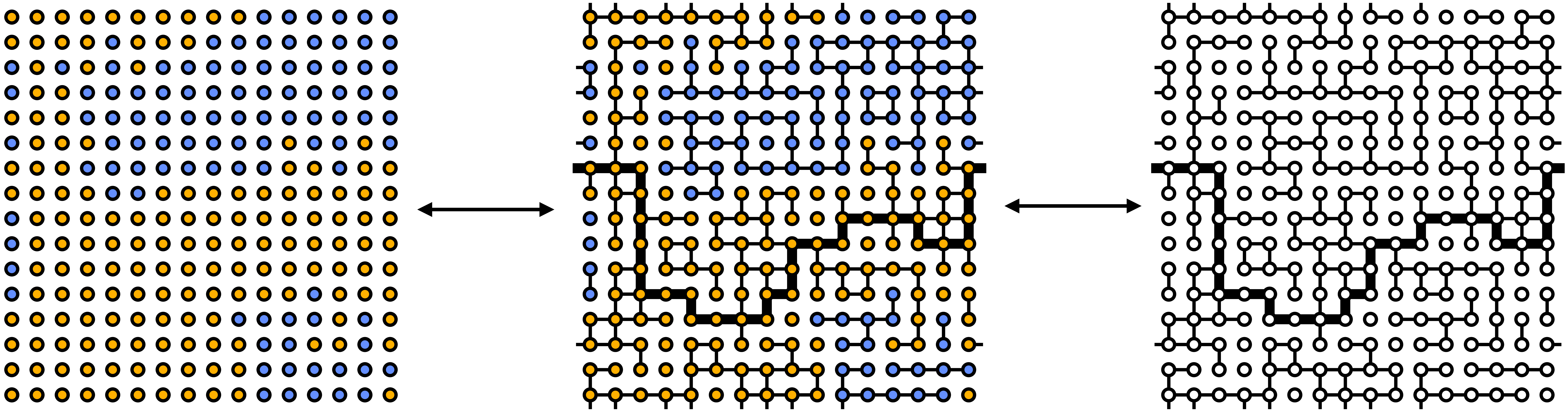

Potts model — *~~ topology ~~* — *random-cluster model*

We use topology to generalize important physical models and the algorithms that simulate them.

preprint `arxiv:2507.13503`

software `github.com/apizzimenti/ATEAMS`

Multicover Bifilt.

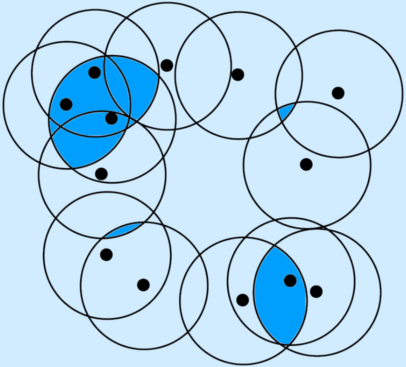

Core Bifiltration

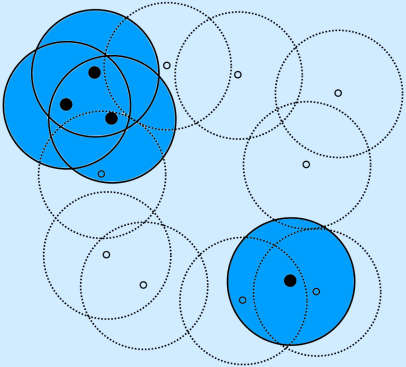

. . .

Variability of topological features of resting-state fMRI networks and clustering approaches with topological data analysis.

Díaz-Patiño J. C.[1], Arelio, I.[1], Alcauter S.[2]

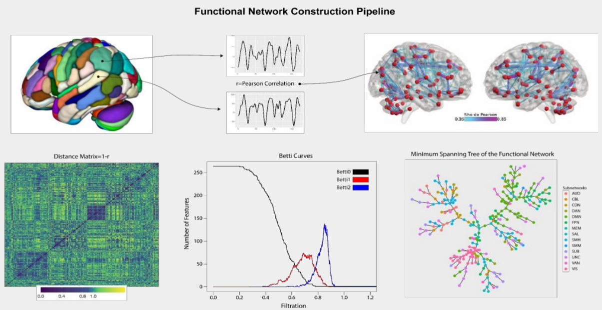

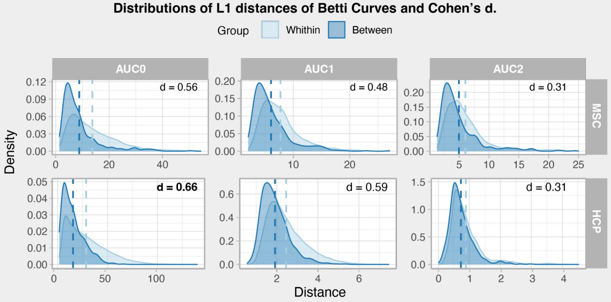

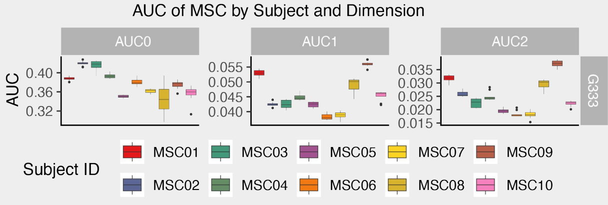

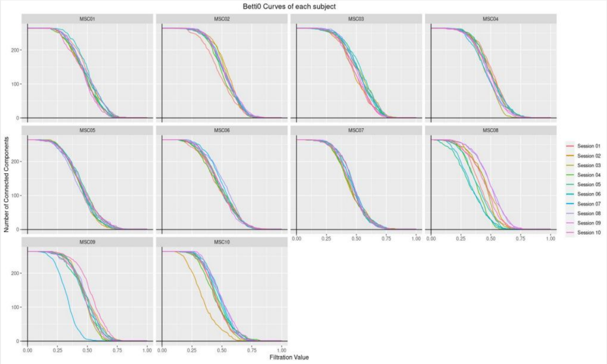

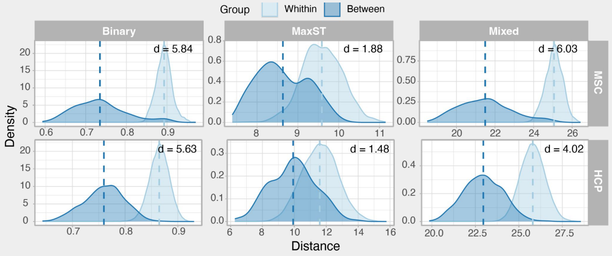

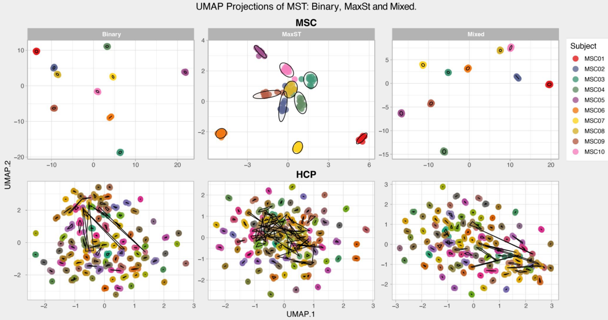

Characterizing Human Brain Activity with Mapper

Ethan Rooke[1], Dorit Kliemann[1], Lisa Byrge[2], Dan P. Kennedy[3], James Traer[1]
The University of Iowa[1], University of North Florida[2], Indiana University[3]

fMRI Data

- 148 Participants, 50 autistic
- 1 hour of short films of various genres
- Samples every 0.72 seconds

Pipeline

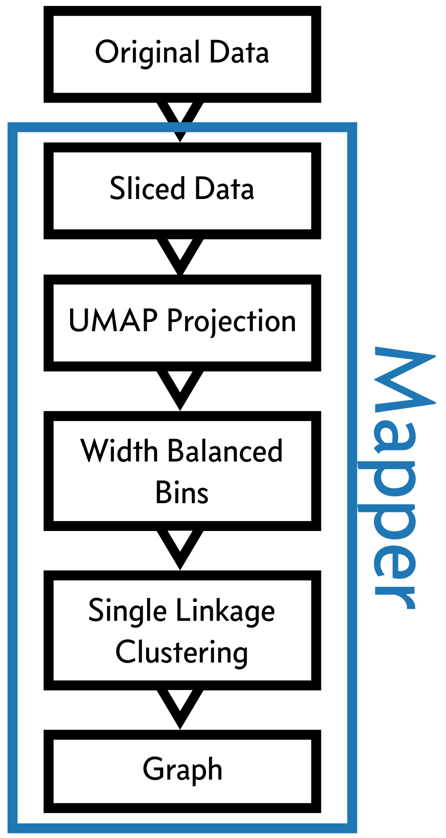

Slicing

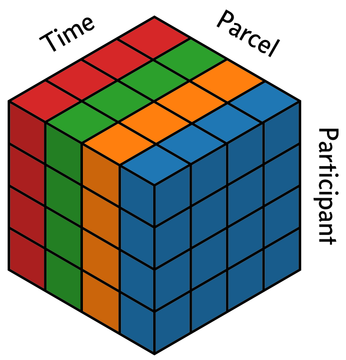

Slicing by Participant

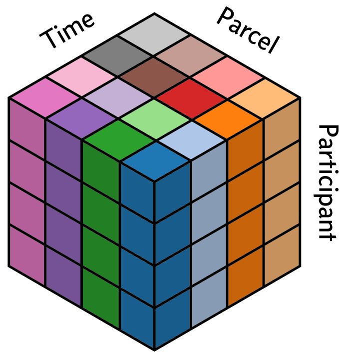

Slicing by Time-Parcel

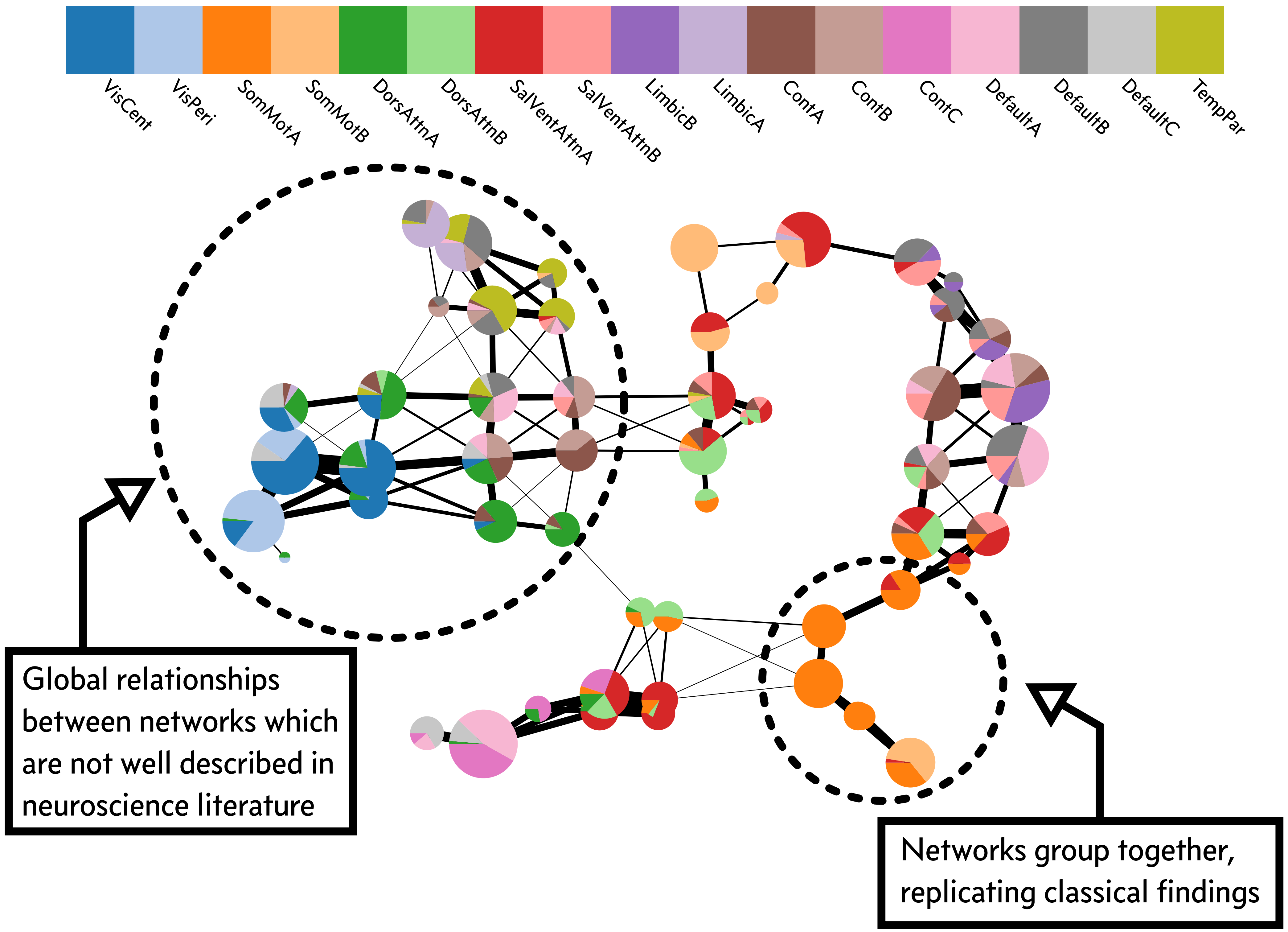

IOWA

Spectral Stability of Persistent Laplacians

Unify setting for Laplacians using **operator theory**

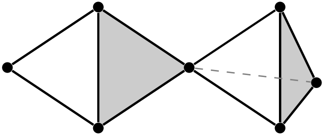

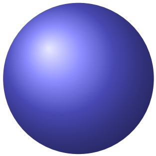

$$\cdots \longrightarrow C_{k+1} \underset{(d_{k+1})^*}{\overset{d_{k+1}}{\rightleftarrows}} C_k \underset{(d_k)^*}{\overset{d_k}{\rightleftarrows}} C_{k-1} \longrightarrow \cdots$$

$$\Delta_k := \underbrace{d_{k+1}(d_{k+1})^*}_{\Delta_{+,k}} + \underbrace{(d_k)^* d_k}_{\Delta_{-,k}}$$

Transfer notion of **persistent Laplacians** to this setting

Extend and **discuss** existing **stability results**

idea: small changes of chain complex should lead to small changes of spectrum

Lightning Talk

- A persistence module is a functor $f : \{0, 1, \ldots, m\} \to R\mathrm{-Mod}$
- This consists of a sequence $\{f_i\}_i$ of R-modules with "structure maps" $\{f(i \leq j) : f_i \to f_j\}_{i,j}$
- An interval decomposition of f is a choice of bases $\beta_i \subseteq f_i$ such that $f(i \leq j)$ maps $\beta_i \setminus \ker(f(i \leq j))$ injectively into β_j
- Interval decompositions always exist when considering field coefficients
- Persistence modules arise naturally from PH
  - $\mathcal{K}_0 \subseteq \mathcal{K}_1 \subseteq \mathcal{K}_2 \subseteq \cdots \subseteq \mathcal{K}_m$
  - $H_k(\mathcal{K}_0) \to H_k(\mathcal{K}_1) \to H_k(\mathcal{K}_2) \to \cdots \to H_k(\mathcal{K}_m)$
  - interval decompositions provide information for persistence diagrams

Theorem (L., Henselman-Petrusek)

Let f be a persistence module that is pointwise free and finitely-generated over a PID. Then f splits into a direct sum of interval modules if and only if the cokernel of every structure map $f(i \leq j)$ is free.

Six-packs of persistence diagrams for chromatic point sets

Ondřej Draganov

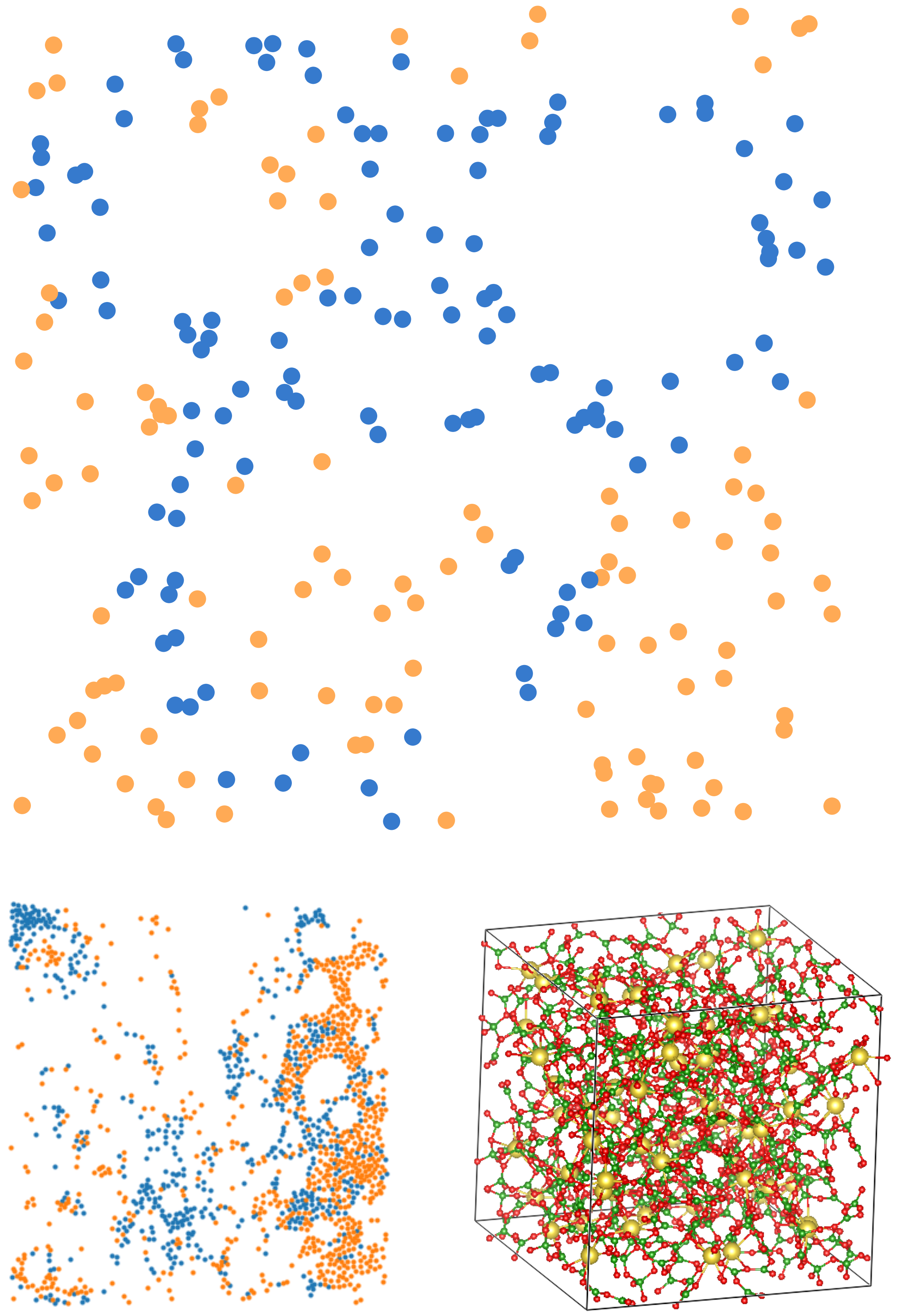

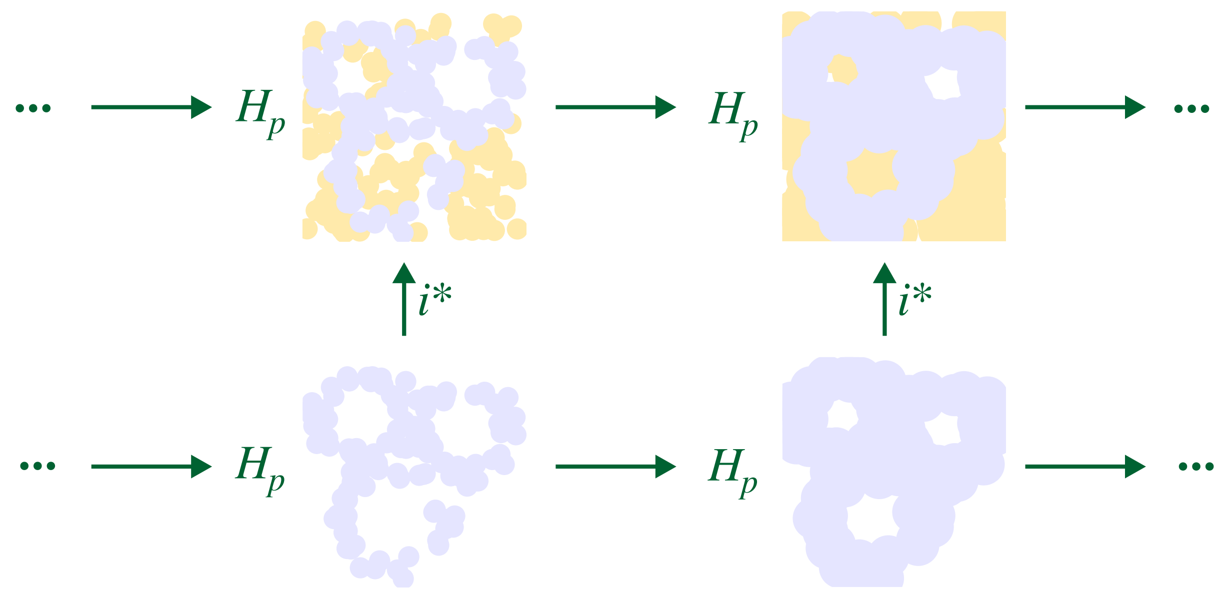

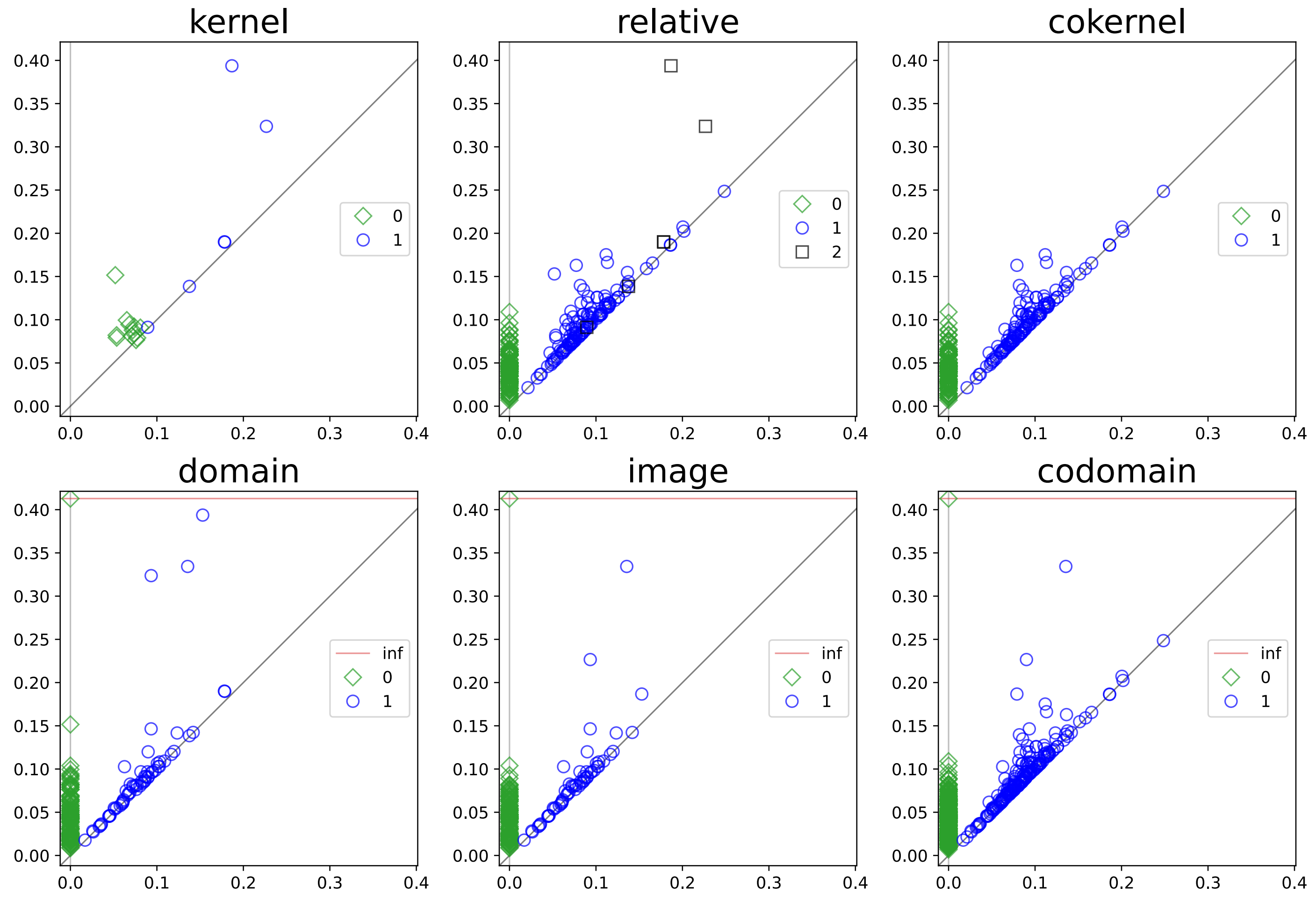

16: Topological Data Analysis distinguishes gut microbiome profiles of Parkinson's disease mouse models

Eva Lymberopoulos

UCL

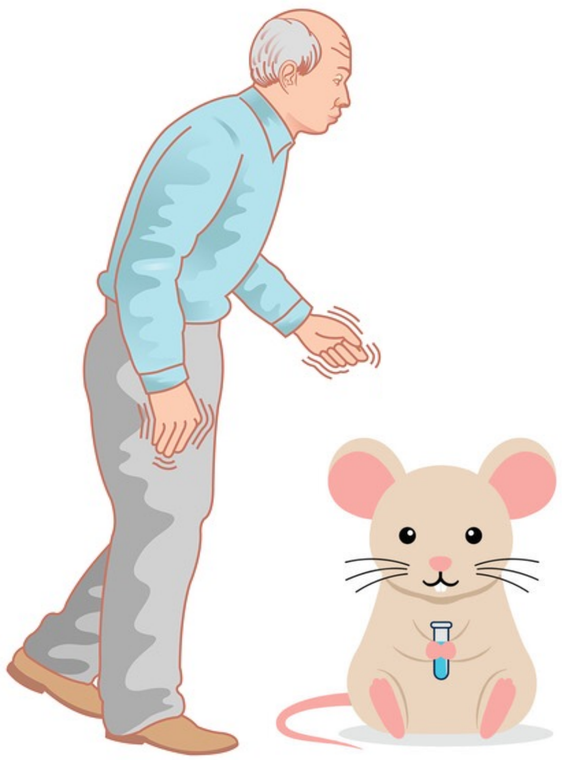

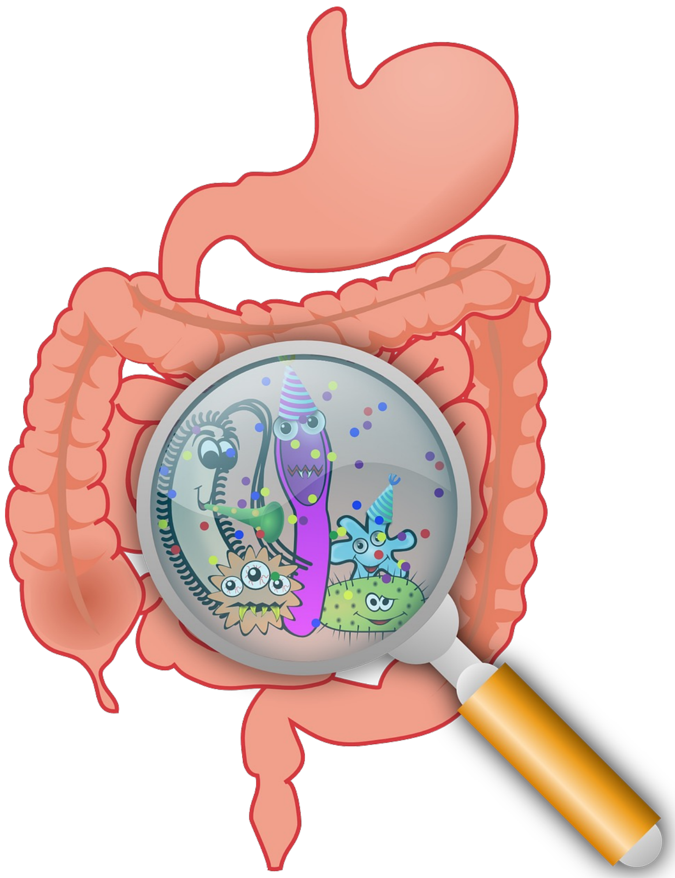

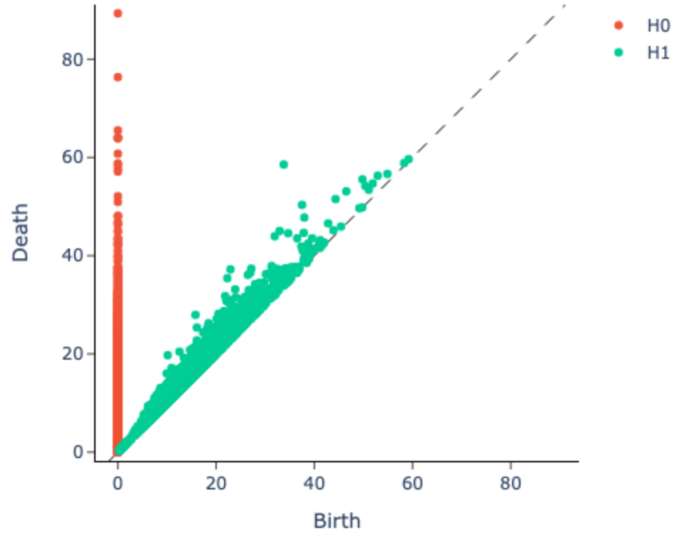

biocortex

Unveiling Topological Structures from Language: A Comprehensive Survey of TDA Applications in NLP

Adaku Uchendu, joint work with Thai Le

- **Theoretical Approaches**
  - **TDA techniques that probe text or speech to reveal or confirm linguistic phenomena**

- **Non-theoretical Approaches**
  - **TDA techniques that improve or explain model performance**

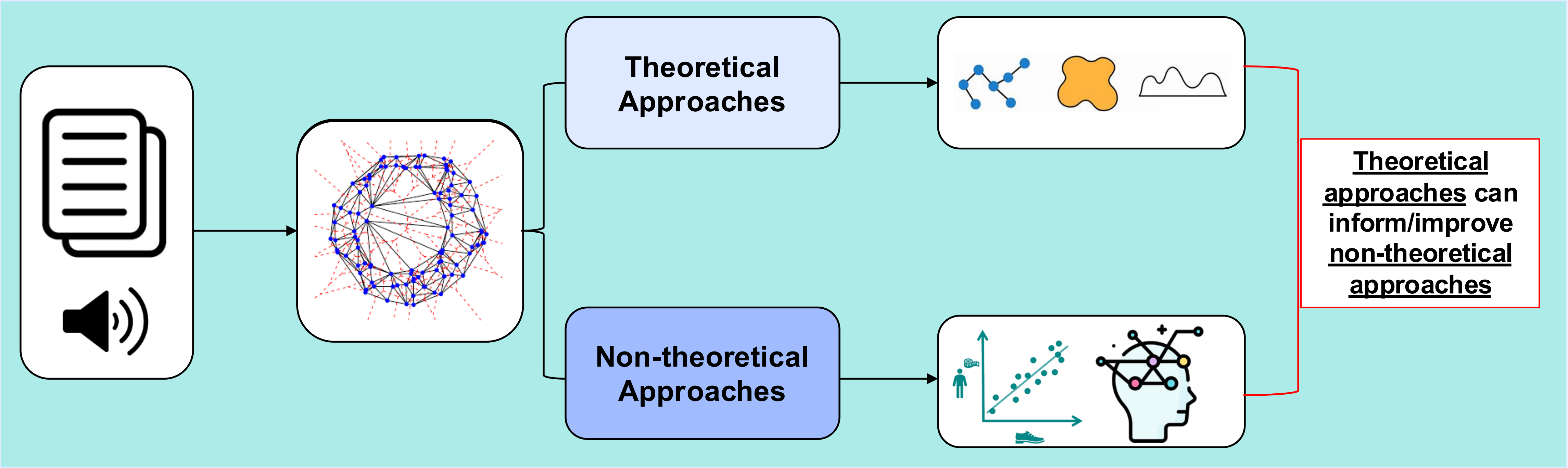

Gromov-Hausdorff distance to compare chromatic metric spaces

Ondřej Draganov, Sophie Rosenmeier, **Nicolò Zava**

poster n. 18

Datasets and shapes

Metric spaces

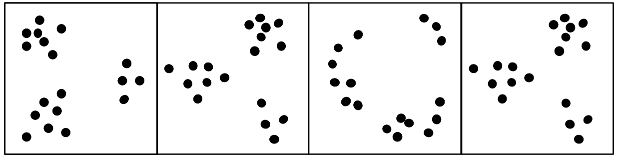

Metric spaces with colours, labels, features

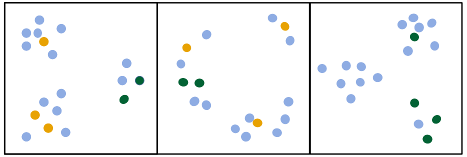

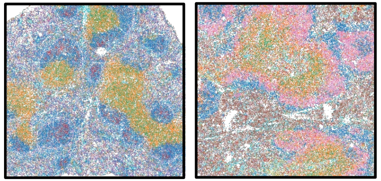

Gromov-Hausdorff distance

STABILITY

***C*-constrained Gromov-Hausdorff distance**

STABILITY

Topological and metric invariants

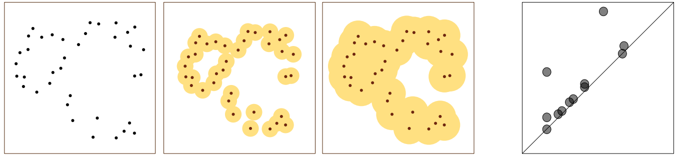

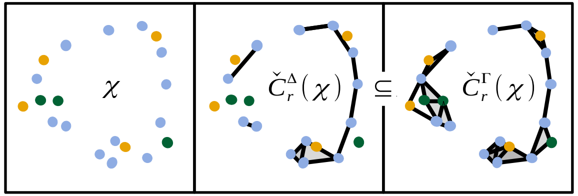

$$\begin{tikzcd}
{} \arrow[r] & \check{C}^{\Gamma}_{r}(\chi) \arrow[r] & \check{C}^{\Gamma}_{s}(\chi) \arrow[r] & {} \\
{} \arrow[r] & \check{C}^{\Delta}_{r}(\chi) \arrow[r] \arrow[u] & \check{C}^{\Delta}_{s}(\chi) \arrow[r] \arrow[u] & {}
\end{tikzcd}$$

Six-pack

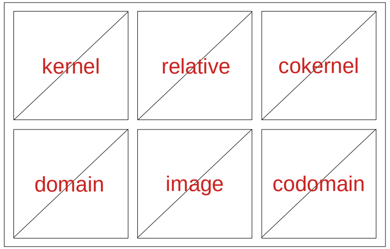

Knot Data Analysis Using Goeritz Invariants

We propose a point cloud data analysis method using the Goeritz invariant, one of the invariants in knot theory.”

1.Point Cloud Data

- **Point cloud**: a set of many discrete points distributed in space
- **Examples**: Atomic arrangements, CT images, Protein structure data
- **Studies**: Topological data analysis (TDA) has been used to extract geometric features from point cloud data

2.Goeritz Invariant

- We propose a method to extract knot information from simplicial complexes constructed by expanding point cloud data through filtration.
- The Goeritz invariant, which we apply to knot data analysis, is a topological invariant computed based on the crossings of knots.

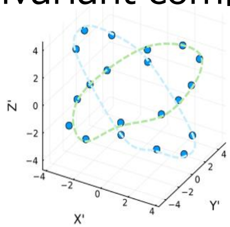

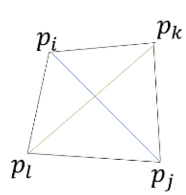

3.Result of Experiment

- The proposed KDA method can distinguish between two types of synthetic point clouds that cannot be distinguished by conventional TDA

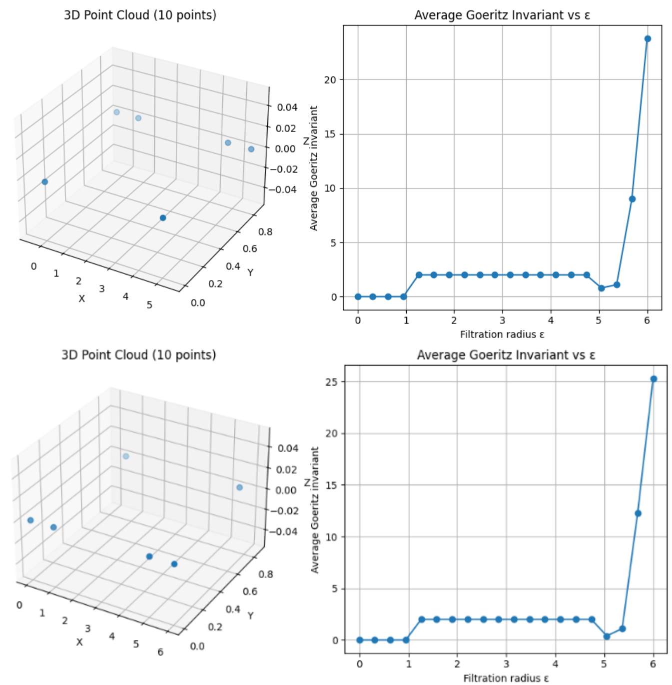

Tatsuya Matsuba
Institute of Science Tokyo, School of Engineering, Doctoral Course